Journal of Power Sources 195 (2010) 2579–2585

Contents lists available at ScienceDirect

Journal of Power Sources

journal homepage: www.elsevier.com/locate/jpowsour

# Development of a proton exchange membrane fuel cell cogeneration system

Jenn Jiang Hwang*, Meng Lin Zou

*Department of Greenergy, National University of Tainan, Tainan 700, Taiwan*

ARTICLE INFO

*Article history:*
Received 8 September 2009
Received in revised form 28 October 2009
Accepted 28 October 2009
Available online 2 December 2009

*Keywords:*
Proton exchange membrane fuel cell
Cogeneration
Efficiency

ABSTRACT

A proton exchange membrane fuel cell (PEMFC) cogeneration system that provides high-quality electricity and hot water has been developed. A specially designed thermal management system together with a microcontroller embedded with appropriate control algorithm is integrated into a PEM fuel cell system. The thermal management system does not only control the fuel cell operation temperature but also recover the heat dissipated by FC stack. The dynamic behaviors of thermal and electrical characteristics are presented to verify the stability of the fuel cell cogeneration system. In addition, the reliability of the fuel cell cogeneration system is proved by one-day demonstration that deals with the daily power demand in a typical family. Finally, the effects of external loads on the efficiencies of the fuel cell cogeneration system are examined. Results reveal that the maximum system efficiency was as high as 81% when combining heat and power.



## 1. Introduction

From the viewpoints of energy saving and reduction in greenhouse gas emission, the fuel cell has been drawing attention as the next-generation power source [1–4]. In recent years, automobile manufacturers have been vigorously developing proton exchange membrane (PEM) fuel cells as propulsion sources of electric vehicles on account of its good start-up performance due to a relatively low operating temperature and its high power density [5,6]. PEM fuel cell is also promising for residential cogeneration systems since it is very efficient in converting fuel gas into useful energy by recovering the waste heat from the electricity generation, which is used to heat domestic hot water and/or for central heating of the home [7–15]. In addition, the electricity is generated in the home and hence there is no transmission loss associated with central power generation.

The present paper relates to a fuel cell cogeneration system generating electric power and hot water. It is an extension of the author's previous work about the fuel cell system for vehicle propulsion [5]. In the previous work, the heat generated by the chemical reaction of fuel cells is dissipated to the atmosphere by using a radiator together with a cooling fan. In contrast, the present fuel cell cogeneration system recoveries the waste heat from the fuel cell as useful hot water. This recovered heat is initially stored in a storage tank, and then is used as a hot water supply or for room heating.

The objective of the present study is to design, fabricate, and demonstrate a fuel cell cogeneration system. First, subsystems of the fuel cell cogeneration system, including hydrogen delivery subsystem, air delivery subsystem, power management subsystem and regeneration subsystem, are assembled and tested. Then, a single-chip microcontroller embedded with smart algorithm is developed that integrates the above subsystems and a commercial 5-kW PEM fuel cell stack [5] into a fuel cell cogeneration system. Subsequently, the stability of the fuel cell cogeneration system is verified by checking the electrical and thermal dynamic behaviors under constant loads. Its reliability and durability is further demonstrated by supporting the daily power demands of a typical family. Operation strategies for stand-alone and grid-connected applications of the fuel cell cogeneration system are proposed and compared thereafter. Finally, the effect of external loads on the system efficiencies, including electrical efficiency, heat recovery efficiency, and combined heat and power efficiency, is examined and discussed.

## 2. Experiments

A schematic drawing of the PEM fuel cell cogeneration system is shown in Fig. 1. It consists a PEM fuel cell stack, an air delivery subsystem (green circuit), a hydrogen delivery subsystem (blue circuit), a power management subsystem (black circuit), and a regeneration subsystem. (For interpretation of the references to color in this sentence, the reader is referred to the web version of the article.) Except for the regeneration subsystem, the fabrication

* Corresponding author at: Department of Greenergy, National University of Tainan, 33, Sec. 2, Su-Lin St., Tainan 700, Taiwan. Tel.: +886 62600321; fax: +886 62602251/62602596.
*E-mail address:* azaijj@mail.nutn.edu.tw (J.J. Hwang).

0378-7753/$ – see front matter © 2009 Elsevier B.V. All rights reserved.
doi:10.1016/j.jpowsour.2009.10.087

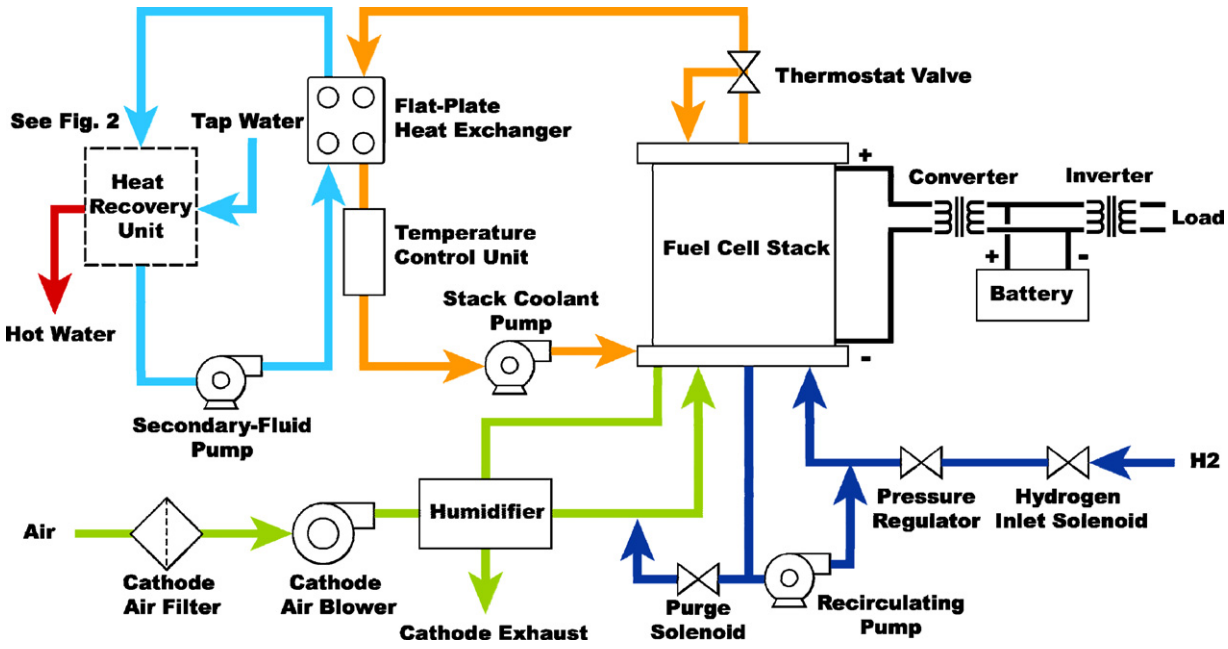


**Fig. 1.** Block diagram of the fuel cell cogeneration system.

of the other subsystems has been described in detail elsewhere [5]. Only some important features are stressed below.

### 2.1. Air delivery subsystem

The air delivery subsystem provides filtered, conditioned air to the fuel cell stack. The major components are the cathode air filter, cathode air blower and humidifier. The cathode air filter removes particulate and chemical contaminates from the airstream. The cathode air blower controls the airflow rate to the stack. The speed of the blower is variable that is a function of DC output of the fuel cell stack. The humidifier transfers heat and humidity from the stack outlet gases to the inlet airstream. It has no moving parts and uses membrane material to exchange heat and moisture between the incoming and outgoing airstreams.

### 2.2. Hydrogen delivery subsystem

The fuel cell cogeneration system is fueled by hydrogen at the inlet pressure range of 4.0–7.0 atm. A normally closed hydrogen inlet solenoid valve allows hydrogen flow into the system, which is actuated by 24VDC solenoid coil. The pressure regulator reduces incoming hydrogen pressure (i.e., 4.0–7.0 atm) to 1.02 atm. A recirculating pump circulates unused hydrogen from the anode exit to

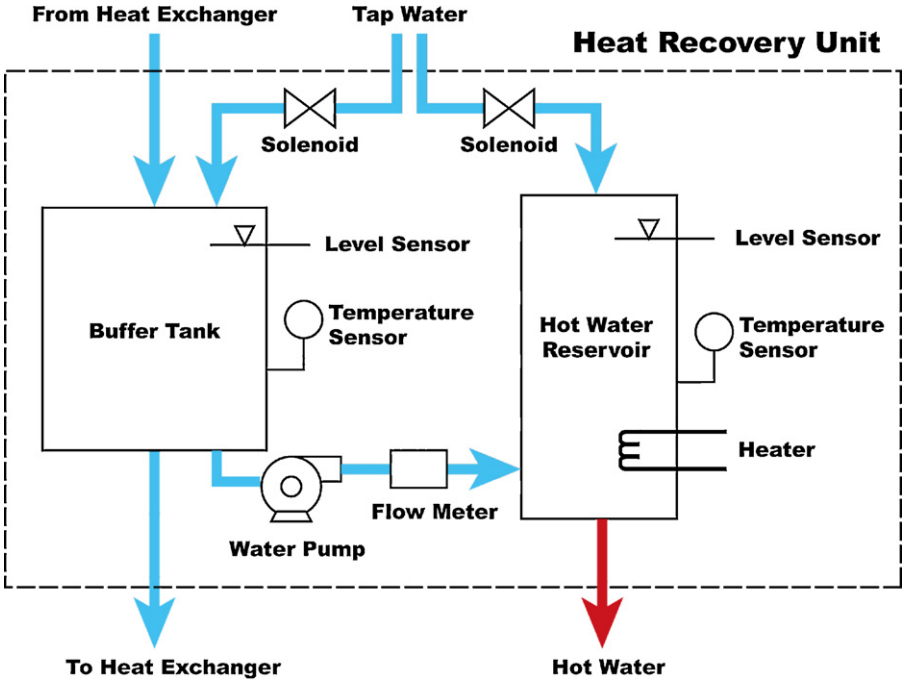


**Fig. 2.** Schematic drawing of the heat recovery unit.

the anode inlet. The hydrogen pipeline in the present system is designed as a dead end. The anode hydrogen pressure decreases gradually due to the hydrogen oxidation reaction (HOR). The feeding of hydrogen in the anode depends on the anode hydrogen pressure. That is when the anode pressure is lower than a predetermined value, e.g., 1.01 atm, the inlet solenoid valve opens to feed the anode with fresh hydrogen that increases the hydrogen pressure. When the hydrogen pressure increases to a predetermined value, e.g., 1.02 atm, the inlet solenoid value is closed. Then, the anode pressure decreases again due to HOR. As a result, the anode hydrogen pressure always keeps in the range of 1.01–1.02 atm by switching the inlet solenoid valves on/off again and again.

### 2.3. Power management subsystem

The power management subsystem manages the output power to the external load as well as the auxiliary power for the system. It is composed of a battery bank, DC/DC converters and DC/AC inverters. Two DC/DC converters condition the stack output to provide positive 24VDC and 48VDC for auxiliary power and external load, respectively. The 48VDC is then converted to110VAC (alternating current) by the inverter and subsequently supplied to external loads.

### 2.4. Regeneration subsystem

The regeneration subsystem has two fluid circuits, i.e., stack coolant circuit (orange) and secondary-fluid circuit (light blue). The stack coolant circuit is filled with a nonconductive heat transfer fluid, uninhibited propylene glycol/DI water mixture (55%/45%). During normal operation, the stack coolant pump circulates coolant at constant speeds through the fuel cell stack to remove the heat dissipated by the fuel cell stack. The stack coolant pump is a combination of a 24VDC motor with magnetic-drive seal-less head and ceramic impellers. It operates when the fuel cell system is operating. A thermostat controls the coolant flow through the heat exchanger while maintaining constant flow through the stack. The excess heat in coolant is then transferred to the secondary fluid that is circulated by a variable speed pump to control heat transfer. The secondary fluid used here is tap water. A temperature sensor [16] monitors the coolant temperature and provides to feedback to control the speed of the secondary-fluid pump. In the present work, the stack coolant inlet temperature (SCIT) is controlled to 57 °C that ensures the fuel cell operation temperature around 80 °C. Note that the simulation results revealed that the temperature difference between the reaction site and the coolant contact boundary in a PEM fuel cell can be up to 20 °C [17–19].

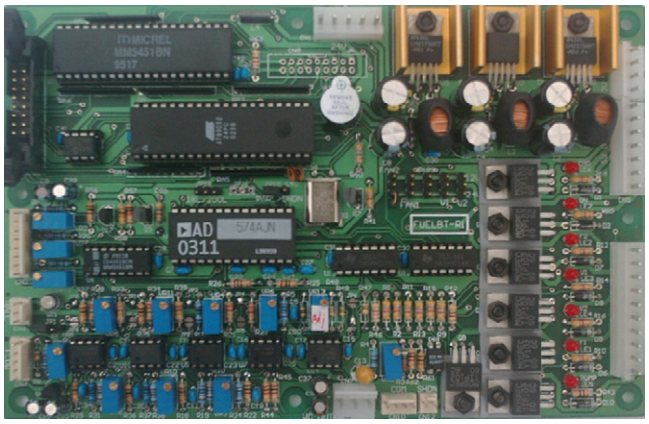

**Fig. 3.** Single-chip microcontroller of the fuel cell cogeneration system.

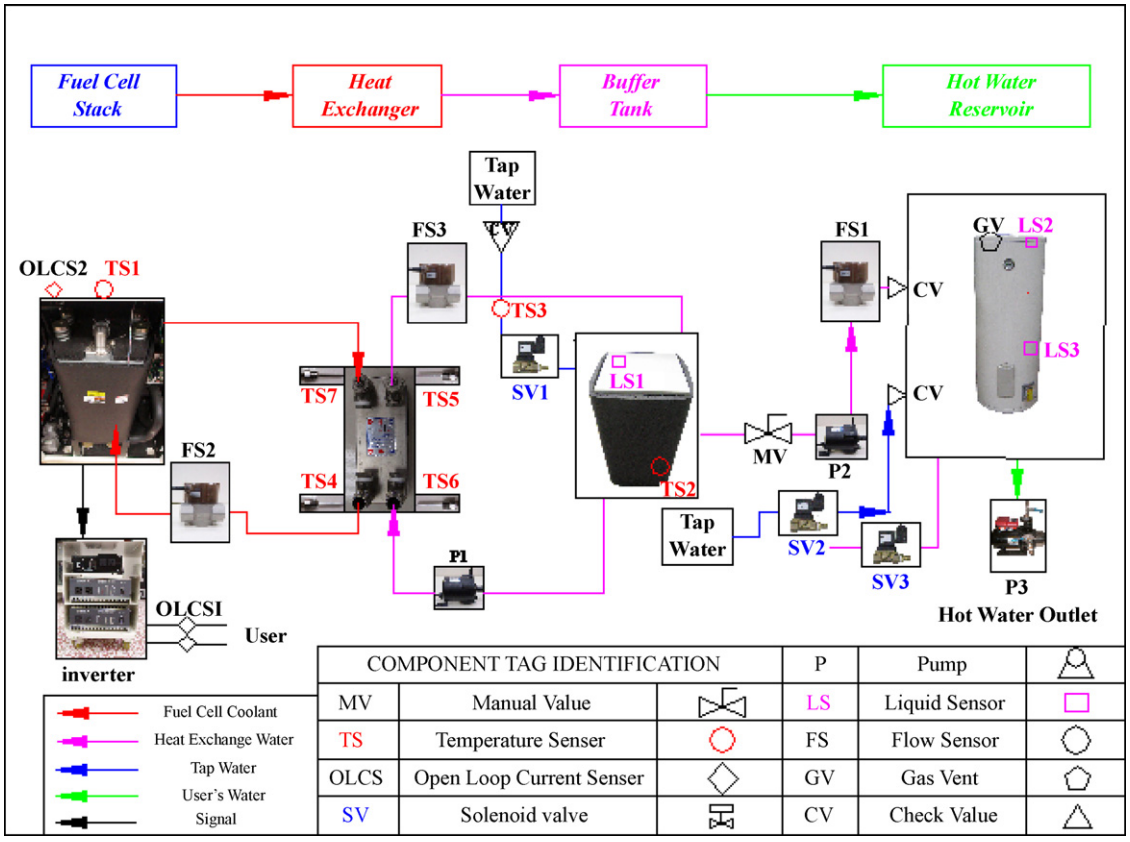


**Fig. 4.** View of the man–machine interface of the fuel cell cogeneration system.

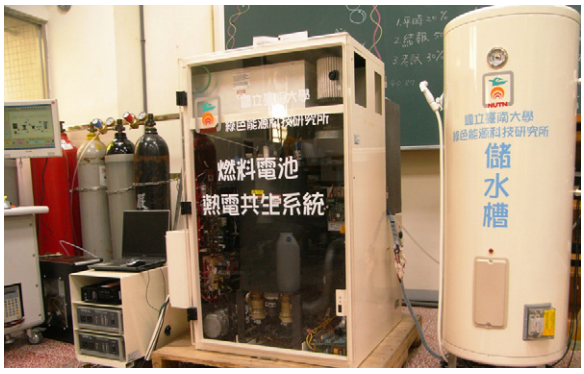


**Fig. 5.** Photo of the present fuel cell cogeneration system.

The heat dissipated by the fuel cell is recovered into useful energy in the heat recovery unit (dashed block). The details of the heat recovery unit are given in Fig. 2. The water temperature in the buffer tank gradually increases during operation. When it reaches a predetermined value (known as heat-recovery temperature), say 50 °C, the water pump begins impelling the hot water from the buffer tank to a hot-water reservoir. Simultaneously, tap water is poured into the buffer tank to keep the water level of the buffer tank. It stops impelling the hot water when the water temperature in the buffer tank reduces to a predetermined value, e.g., 48 °C. As a result, the hot-water reservoir receives 48–50 °C tap water from the buffer tank now and then. If the water temperature in the hot-water reservoir decreases to a predetermined value, e.g., 48 °C due to the heat loss, the microcontroller issues a command signal to the fuel cell to supply electric power to the electric heater installed inside the hot-water reservoir. Thus, the fuel cell cogeneration system can always provide hot water of temperature 48–50 °C to end-users.

### 2.5. Microcontroller

As shown in Fig. 3, a single-chip microcontroller together with smart algorithms is developed for controlling the fuel cell cogeneration system under all operation conditions. In the present fuel cell cogeneration system, an Intel 8051 microprocessor is used to govern the system. It is capable of monitoring the sensor signals of voltage, current, temperature, and pressure. It also takes appropriate actions in order to drive the actuation devices such as the cathode air blower, solenoid valves, water pumps, and heaters. All data and parameters are collected and downloaded to a personal computer through the RS232 communication port on the microcontroller. In addition, as shown in Fig. 4, a man–machine interface (MMI) is designed for real-time monitoring the experimental data and operation conditions of the fuel cell cogeneration system.

### 2.6. System integration and assessment

Before integration of the fuel cell cogeneration system, each sensor is calibrated using a laboratory-quality instrument that ensures its accuracy and reliability over the ranges in which it is operated [20]. Also, each actuator such as solenoid valves and relays is tested independently in order to check its availability and performance. Each subsystem is then assembled on a breadboard, and a series of tests is conducted to verify these subsystems. Finally, all subsystems are installed in a designed metallic box for housing the entire system. Fig. 5 shows a photo of the present fuel cell cogeneration system.

Safety is always a matter of concern about hydrogen-powered systems. Before each run, regular leakage checks were conducted for the entire hydrogen pipeline such as connections, fittings, valves and the fuel cell stack. The microcontroller automatically performs a shutdown whenever it detects a parameter out of a prescribed range. During the assembly and testing of the fuel cell cogeneration system, no accidents, hazardous or potentially hazardous situations occurred.

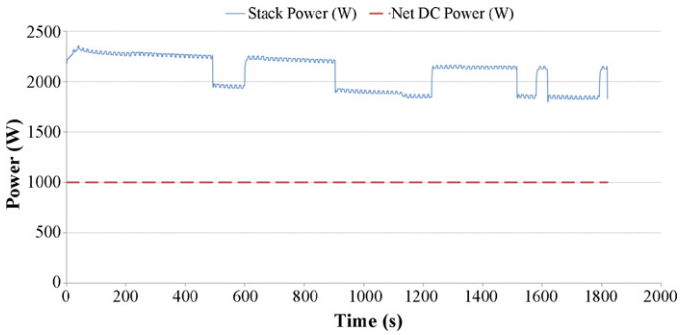


**Fig. 6.** Dynamic behaviors of the stack power under the external load of 1 kW.

## 3. Results and discussion

### 3.1. Power and thermal dynamics

Fig. 6 shows the dynamics of the stack power (blue curve) under a constant external load of 1 kW (i.e., net DC power, red dashed line). (For interpretation of the references to color in this sentence, the reader is referred to the web version of the article.) The stack power is higher than the net DC power by 800–1300 W. The power gap represents the auxiliary consumptions and the transmission/conversion losses in the electrical circuit. Note that the step change in the stack-power distribution is mainly caused by the operation of the cathode air blower. The power demand of the air blower is dependent not only on the load operation but also on the cell voltage. When the cell voltage decreases to an extent, e.g., 0.4 V per cell, the air blower should run in full power modes to blow out the accumulated water inside the electrode. Therefore, the power step is due to the action of the air blower. In addition, the stack power goes down with time is because the power requirement for charging the secondary battery is reduced gradually. Due to the space limitation, the hybridization of the fuel cell and the secondary battery will be discussed in our future effort.

Fig. 7 shows the dynamics of the stack coolant inlet temperature (SCIT) under the external load of 1 kW. It is seen that the SCIT keeps in the range of $57 \pm 2$ °C that guarantees proper operation temperature of the fuel cell [17–19]. The high frequency of temperature fluctuation in this figure is coincident with by the PWM frequency of the secondary-fluid pump, which is also shown by little ripples on the stack-power distribution in Fig. 6.

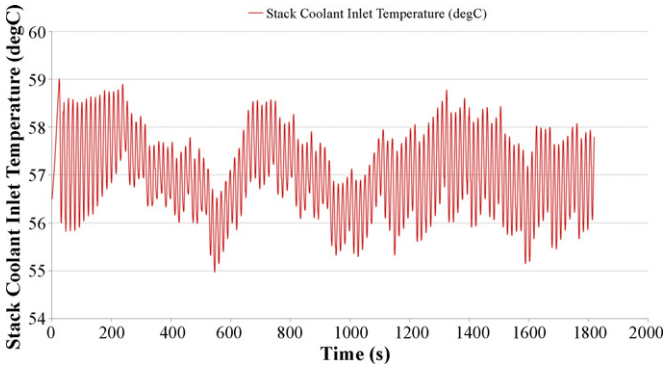


**Fig. 7.** Dynamic behaviors of the stack coolant inlet temperature.

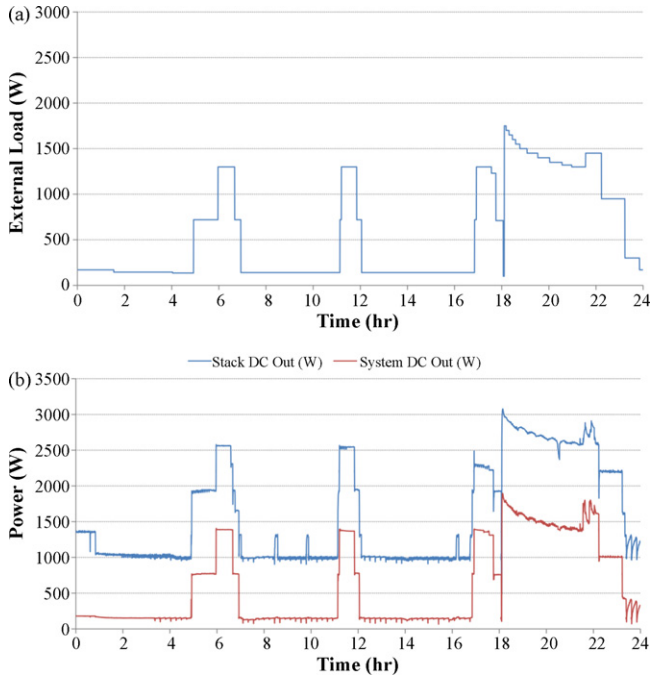


**Fig. 8.** (a) Model of daily power demand of a typical family, and (b) dynamic responses of the stack/system powers of the fuel cell cogeneration system.

### 3.2. Demonstration of a stand-alone cogeneration

The present fuel cell cogeneration system is designed for residential or commercial purposes. It can serve as a stand-alone power supply or feed in the grid. To meet the user power demand on a daily life, it is important to verify the reliability and stability of the present fuel cell cogeneration on a large variation of load encountered in real applications, e.g., system start and stop, and step change in load. The dynamic characteristics of the present fuel cell cogeneration system responding to simulated daily power consumptions of a family are presented in the following discussion.

Fig. 8(a) models the daily power demands of a typical family. From the midnight to early morning (00:00–05:00) all families are sleeping and thus the power requirement is low that keeps the household electronics and appliances, such as refrigerators and safety lighting. In the morning (05:00–07:00), at noon (11:00–12:00), and in the early evening (17:00–18:00), more power is required for cooking, leisure, reading, etc. From the evening to midnight (18:00–23:00), the consumption of electric power is considerable due to family activities.

Fig. 8(b) shows the responses of the fuel cell cogeneration system to the daily power demands in Fig. 8(a). The red curve is the net DC power delivered by the system while the blue curve represents the stack power. (For interpretation of the references to color in this sentence, the reader is referred to the web version of the article.) Again, the gap between these two curves is the power dissipations by auxiliaries together with the transmission/conversion losses. As shown in Fig. 8(b), the fuel cell cogeneration system works well in all day long. There are no failures during operation. Even with a steep variation of external loads, such as at 18:00 the external power drops suddenly from 750 W to 200 W and immediately goes up to 1800 W, the present fuel cell cogeneration system still works properly and normally.

Attention is turning to the regeneration subsystem for recovering the hot water. Fig. 9 shows the flow rates of hot water from the buffer tank to the hot-water reservoir. According to the control algorithm, the water pump in Fig. 2 begins/stops impelling the hot water when the temperature of the hot water in the buffer tank

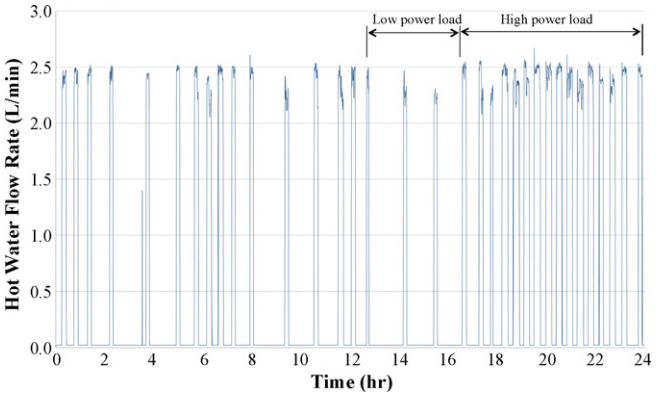


**Fig. 9.** Hot-water flow rates from the buffer tank to the hot-water reservoir.

increases higher/reduces lower than 50 °C/48 °C. This ensures that the hot water entering the hot-water reservoir keeps at 49 ± 1 °C. Basically, the frequency of pumping hot water is dependent on the electric power delivered by the fuel cell stack. It is interesting to note that more hot water is produced at higher electrical power consumption levels. The amount of hot water produced by the cogeneration system is about 1830 L on a daily basis. Previous results [20] showed that the average daily use of hot water (50 °C) for male and female are above 50 L per person and 80 L per person, respectively. Therefore, a 4-people family needs about 230–290 L hot water per day. Apparently, the present fuel cell cogeneration system produces much more hot water than that for home use based on the above operational strategy.

Fig. 10 further shows the effect of external loads on the production rate of hot water in the present fuel cell cogeneration system. The diamond symbols are the experiment data, whereas the dashed line represents the curve-fitting results. It is seen from this figure that the hot-water production rate increases with increasing the external load. Taking an example of the external load of 1.5 kW, it can produce about 80 L hot water per hour. That is, 4-h operation of the cogeneration system can support the daily hot-water requirement in a typical family.

### 3.3. Application of grid-connected cogeneration

In order to optimize the generation of electric power and the production hot water for home use, an operation strategy of the present fuel cell cogeneration system is proposed by considering public utilities. Fig. 11 shows the operation strategy of the present fuel cell cogeneration if the grid simultaneously provides the elec-

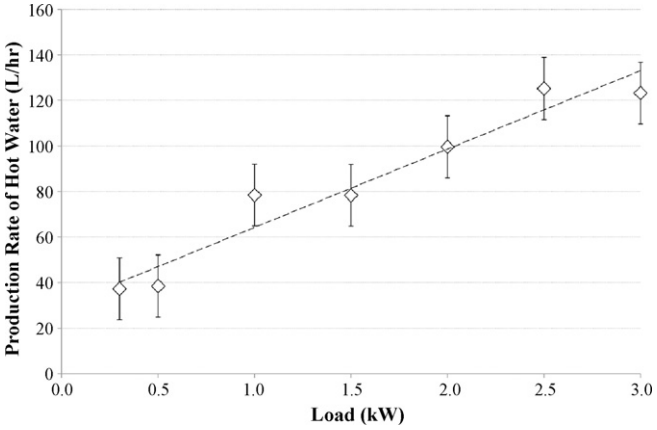


**Fig. 10.** Effect of external load on the production rate of hot water.

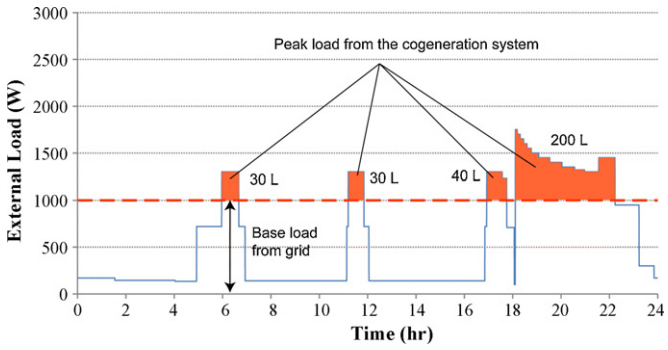


**Fig. 11.** Operation strategies for the grid-connected fuel cell cogeneration system.

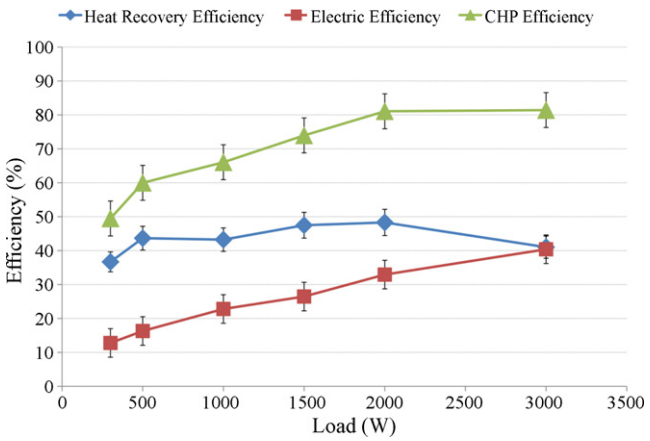


**Fig. 12.** Effect of external load on the efficiencies of the fuel cell cogeneration system.

tric power for the family power demands (Fig. 8(a)). As shown in Fig. 11, on the off-peak stages, the grid supplies the electric power to the user power demand, while the fuel cell cogeneration system keeps off. In the peak-power periods, the grid provides the base load up to 1 kW (red dashed line), and the deficiency of power is offset by the fuel cell cogeneration system (orange shade block). (For interpretation of the references to color in this sentence, the reader is referred to the web version of the article.) As indicated in Fig. 11, about 300 L hot water is produced by the fuel cell cogeneration system which is enough to support the daily need for a family. Noteworthy that the economic significance of the above application is not only the high system efficiency by producing useful hot water but also highly valued electric power generated in peak-power periods. Moreover, surplus electric power produced by the fuel cell cogeneration system could feed into the grid to relax the pressure of high power demand in the peak periods.

### 3.4. Efficiencies of the cogeneration system

The electrical efficiency of the fuel cell cogeneration system can be determined by accounting for the stack power, auxiliary power consumption and power conversion/transmission loss. Table 1 lists the electric features of the major auxiliary components in the fuel cell cogeneration system. The present work, however, does not use this approach since it is difficult to accurately determine the efficiency of each power conversion device and the power consumption of supported components. For example, it is hard to catch the real power dissipation by the temperature-dependent pump, which fluctuates by the speed-up and the slow-down of the motor during the operation. The efficiency is herein defined as the ratio of the net power delivered to external load from the fuel cell cogeneration system to the enthalpy flow (lower heating value) of the consumed hydrogen, i.e.,

$$\varepsilon_E = \frac{P_L}{P_{H_2}} = \frac{I \times V}{n_{H_2} \times \Delta h} \quad (1)$$

where $P_L$ is the net power output to the external load from the fuel cell that is a direct measure of voltage ($V$) across the external load and the current ($I$) passing through the circuit. As for $P_{H_2}$, it is hard to directly measure the hydrogen consumption rate ($n_{H_2}$) in the fuel cell anode. An alternative method to determine the hydrogen consumption rate is given below. The hydrogen oxidation reaction in the anode of a fuel cell is:

$$H_2 \rightarrow 2H^+ + 2e^- \quad (2)$$

Therefore, the hydrogen consumption rate is proportional to the protons (also current) through the fuel cell during reaction. That is the current passing through the fuel cell can represent the hydrogen consumption rate:

$$\varepsilon_E = \frac{I \times V}{0.5 \times I \times N \times C \times \Delta h} \quad (3)$$

where $N$ is the number of the cells in the stack and $C$ is a transfer coefficient between the hydrogen consumption rate and current, i.e., 0.6267 mg $H_2$ $A^{-1}$ $min^{-1}$. The heat recovery efficiency is defined as the ratio of heat recovered by the secondary fluid (tap water) to the hydrogen energy consumption. That is,

$$\varepsilon_T = \frac{P_{water}}{P_{H_2}} = \frac{m_{H_2O} c_{H_2O}\ \Delta T}{0.5I \times N \times C \times \Delta h} \quad (4)$$

where $m_{H_2O}$ (kg $s^{-1}$) is the mass flow rate of hot water, $c_{H_2O}$, the specific heat of water (kJ $kg^{-1}$ $K^{-1}$), and $\Delta T$, the water temperature difference (K).

The combined heat and power (CHP) efficiency in the present cogeneration is:

$$\varepsilon_{CHP} = \varepsilon_T + \varepsilon_E \quad (5)$$

Fig. 12 shows the efficiencies of the fuel cell cogeneration system as a function of the external load. The general trend of the electrical efficiency is an increase of $\varepsilon_E$ with increasing external load. It compares well to test results from other researches made on fuel cell systems [21] and the author's previous work [5]. It is interesting to note that the commercial non-cogeneration FC system, Plug Power GenCore, shows an electrical efficiency above 35% (HHV) for most of the power demand. The difference of the electrical efficiency between the present cogeneration FC unit and the standard FC unit

**Table 1**
Typical power consumption/conversion efficiency of the major components/devices of the fuel cell cogeneration system.

| Components | Quantity | Electric specification | Maximum power consumption | Conversion efficiency |
|---|---|---|---|---|
| Cathode air blower | 1 | 24VDC/20 A | 480 W | – |
| Solenoid valves | 5 | 24VDC/0.12 A | 6 W | – |
| Water pump | 2 | 24VDC/1.6 A | 40 W | – |
| Coolant pump | 1 | 24VDC/2 A | 48 W | |
| Microcontroller | 1 | 24VDC/1.6 A | 40 W | – |
| Converter I | 1 | FCV–24VDC | – | 95% |
| Converter II | 1 | FCV–48VDC | – | 95% |

may be attributed to the difference in the BOP employed in the systems, e.g., the secondary-fluid pump in the present FC cogeneration system and the radiator fan in the GenCore unit. In addition, the electric heater in the hot-water reservoir should dissipate some electrical power to keep its temperature in the range of $49 \pm 1\,^{\circ}C$ that reduces the electrical efficiency of the FC cogeneration system. The heat recovery efficiency keeps in the range of $42 \pm 6\%$ when the external loads vary from 300 W to 3000 W. It further shows that the CHP efficiency of the FC cogeneration system increases with an increase of the external loads. The maximum CHP efficiency is about 81%.

## 4. Conclusions

The present work has successfully developed and demonstrated a PEM fuel cell cogeneration that provides high-quality electricity and hot water. Informative outcomes and experiences obtained from the design, fabrication and test of this prototype. In addition, control schemes proposed by this work have managed the cogeneration system properly. The major conclusions are drawn below. First, the stability of the fuel cell cogeneration has been proven by the rational dynamic behaviors of electrical and thermal-fluid properties under constant loads. Moreover, one-day demonstration of the fuel cell cogeneration that copes with real power demands in daily life shows reliable operation without any failure. Finally, the efficiency measurements reveal that the electrical efficiency increases with increasing the external load, while the heat recovery efficiency is not so sensitive to the variation of external load. The maximum efficiencies in electricity, heat recovery, and combined heat and power are up to 40%, 48%, and 81%, respectively.

## Acknowledgements

The author professor Jenn Jiang Hwang would like to thank the National Science Council of Taiwan, for financially supporting this research under contract no. NSC 98-2221-E-024-015-MY2.

## References

[1] J.J. Hwang, C.K. Chen, R.F. Savinell, C.C. Liu, J. Wainright, J. Appl. Electrochem. 34 (2004) 217–224.
[2] J.J. Hwang, D.Y. Lai, J. Power Sources 143 (2005) 75–83.
[3] J.J. Hwang, S.D. Wu, L.K. Lai, J. Power Sources 161 (2006) 240–249.
[4] J.J. Hwang, C.K. Chen, D.Y. Lai, J. Power Sources 140 (2005) 235–242.
[5] J.J. Hwang, D.Y. Wang, N.C. Shih, J. Power Source 141 (2005) 108–115.
[6] J.J. Hwang, W.R. Chang, A. Su, Int. J. Hydrogen Energy 33 (2008) 3801–3807.
[7] G. Gigliucci, L. Petruzzi, E. Cerelli, A. Garzisi, A. La Mendola, J. Power Source 131 (2004) 62–68.
[8] C. Wang, Z. Mao, F. Bao, X. Li, X. Xie, Int. J. Hydrogen Energy 30 (2005) 1031–1034.
[9] P.F. van den Oosterkamp, J. Energy Convers. Manage. 47 (2006) 3552–3561.
[10] P. Corbo, F. Migliardini, O. Veneri, J. Energy Convers. Manage. 48 (2007) 2365–2374.
[11] J.J. Hwang, L.K. Lai, W. Wu, W.R. Chang, Int. J. Hydrogen Energy 34 (2009) 9531–9542.
[12] A.D. Hawkes, M.A. Leach, Energy Policy 36 (2008) 1457–1469.
[13] A.R. Korsgaard, M.P. Nielsen, S.K. Kær, Int. J. Hydrogen Energy 33 (2008) 1909–1920.
[14] C. Xie, S. Wang, L. Zhang, S.J. Hu, Int. J. Hydrogen Energy 191 (2009) 433–441.
[15] H. Ren, W. Gao, Y. Ruan, Appl. Therm. Eng. 28 (2008) 514–523.
[16] J.J. Hwang, G.J. Hwang, R.H. Yeh, C.H. Chao, J. Heat Transfer 124 (2002) 120–129.
[17] J.J. Hwang, J. Electrochem. Soc. 153 (2006) A216–A224.
[18] J.J. Hwang, P.Y. Chen, Int. J. Heat Mass Transfer 49 (2006) 2315–2327.
[19] J.J. Hwang, J. Power Sources 164 (2007) 174–181.
[20] W.R. Chang, J.J. Hwang, F.B. Weng, A. Su, J. Power Sources 166 (2007) 149–154.
[21] Home Energy Conservation Guide, Bureau of Energy, Ministry of Economic Affairs, Taiwan, 2006.